

RDP INC WALTHAM MASS

RDP INC WALTHAM MASS F/G 22/2
SATELLITE DATA PROCESSING SYSTEMS AND ACCELEROMETER DENSITY DAT--ETC(U)
APR 80 P W FIORETTI A L MAZZELLA D J LYONS TADA

APR 80 R W FIORETTI, A J MAZZELLA, R J LEONG F19628-78-C-0226

AFGL-TR-80-0247

NL

1 OF 1
Δ71 Δ
132200

END

DATE _____

FILMED
8-8

DTIC

AD A102299

LEVEL II

(12)

(18)

(19)

AFGL TR-80-0247

(6)

SATELLITE DATA PROCESSING SYSTEMS
AND ACCELEROMETER DENSITY DATA BASE.

(10)

Robert W. Fioretti
Andrew J. Mazzella, Jr.
Rebecca J. Leong
Lawrence D. Cox

(11)

30 Apr 80

(12)

129

RDP, Inc.
391 Totten Pond Road
Waltham, Massachusetts 02154

(9)

FINAL REPORT.

1 Sep 1978 — 31 Mar 1980

(15)

F19628-78-C-0226

(16)

6690

(17)

02

Approved for public release, distribution unlimited.

Prepared for:

AIR FORCE GEOPHYSICS LABORATORY
AIR FORCE SYSTEMS COMMAND
UNITED STATES AIR FORCE
HANSCOM AFB, MASSACHUSETTS 01731

SELECTED
JUL 31 1981
S D

409955
81 7 31 078

Qualified requestors may obtain additional copies from the Defense Technical Information Center. All others should apply to the National Technical Information Service.

UNCLASSIFIED

SECURITY CLASSIFICATION OF THIS PAGE (When Data Entered)

REPORT DOCUMENTATION PAGE		READ INSTRUCTIONS BEFORE COMPLETING FORM
1. REPORT NUMBER AFGL-TR-80-0247	2. GOVT ACCESSION NO. AD A102299	3. REPORTING CATALOG NUMBER
4. TITLE (and Subtitle) Satellite Data Processing Systems and Accelerometer Density Data Base		5. TYPE OF REPORT & PERIOD COVERED 1 Sept. 78 - 31 Mar. 80
7. AUTHOR(s) Robert W. Fioretti Andrew J. Mazzella, Jr. Rebecca J. Leong, Lawrence D. Cox		6. PERFORMING ORG. REPORT NUMBER FINAL REPORT
9. PERFORMING ORGANIZATION NAME AND ADDRESS RDP, Inc. 391 Totten Pond Road Waltham, MA 02154		8. CONTRACT OR GRANT NUMBER(s) F19628-78-C-0226
11. CONTROLLING OFFICE NAME AND ADDRESS Air Force Geophysics Laboratory Hanscom AFB, MA 01731 Monitor/Frank Marcos/LKB		10. PROGRAM ELEMENT, PROJECT, TASK AREA & WORK UNIT NUMBERS 62101F 6690 02AC
14. MONITORING AGENCY NAME & ADDRESS (if different from Controlling Office)		12. REPORT DATE 30 April 1980
		13. NUMBER OF PAGES 31
		15. SECURITY CLASS. (of this report) UNCLASSIFIED
		15a. DECLASSIFICATION/DOWNGRADING SCHEDULE
16. DISTRIBUTION STATEMENT (of this Report) Approved for public release; distribution unlimited.		
17. DISTRIBUTION STATEMENT (of the abstract entered in Block 20, if different from Report)		
18. SUPPLEMENTARY NOTES		
19. KEY WORDS (Continue on reverse side if necessary and identify by block number) Data Processing, Accelerometer, Density, Data Base, Regression Modelling.		
20. ABSTRACT (Continue on reverse side if necessary and identify by block number) This report describes the finalization of an extensive neutral atmospheric density data base taken from four satellite accelerometer systems; development of an empirical model of these data, circular orbit processing, AE-C re-entry data and contractual functions in support of the EUVS experiment.		

SECURITY CLASSIFICATION OF THIS PAGE(When Data Entered)

SECURITY CLASSIFICATION OF THIS PAGE(When Data Entered)

FOREWORD

The efforts described herein were performed under contract to the Atmospheric Structure Branch (LKB), Aeronomy Division of the Air Force Geophysics Laboratory (AFGL), Hanscom Air Force Base, Massachusetts.

Accession For	
NTIS GPO	<input checked="" type="checkbox"/>
NSIC	<input type="checkbox"/>
USCIB	<input type="checkbox"/>
USCIB	<input type="checkbox"/>
By	
Distribution/	
Availability Codes	
Dist	Avail and/or Special
A	

Table of Contents

Foreword.....	iii
Table of Contents.....	v
List of Illustrations.....	vi
1. Introduction.....	1
1.1 AE/S3 Data Base.....	1
1.2 New AE-C Orbits.....	3
1.3 Data Base Properties.....	3
2. Model Development.....	6
2.1 J71, J77 and MSIS Comparison..	6
2.2 Empirical Model.....	6
2.3 Results.....	12
3. Other Contract Functions.....	19
3.1 EUVS Experiment Support.....	19
3.2 AE-C Re-Entry Data.....	21
3.3 Circular Orbit Processing.....	21
4. Conclusions.....	22
5. Acknowledgment.....	22
6. References.....	23

List of Illustrations

<u>Figure</u>	<u>Page</u>
1 Distribution of Density Data.....	2
2 Data Distribution as a Function of Geomagnetic Latitude.....	4
3 Data Distribution as a Function of Local Time.....	4
4 Data Distribution as a Function of Geomagnetic Activity.....	4
5 Data Distribution as a Function of Solar Flux.....	5
6 Data Distribution as a Function of Altitude.....	5
7 Data Base at 180 km: Solar Flux, Density, Ratio to J71 Model and Kp as a Function of Time..	7
8 Frequency Distribution of Percent Differences of all Data from J71 Model.....	8
9 Frequency Distribution of Percent Differences of all Data from MSIS Model.....	8
10 Frequency Distribution of Percent Differences of all Data from J77 Model.....	8
11 Frequency Distribution of Percent Differences of 200 km Data from J71 Model.....	9
12 Frequency Distribution of Percent Differences of 200 km Data from MSIS Model.....	9
13 Frequency Distribution of Percent Differences of 200 km Data from J77 Model.....	9
14 Amplitude and Phases of Annual and Semi-Annual Variations of the Data Base.....	13

List of Illustrations (Cont.)

<u>Figure</u>	<u>Page</u>
15 Amplitude and Phases of Diurnal and Terdiurnal Variations of the Data Base.....	14
16 Semi-Annual Density Variation for each Model at 200 km for 0 Degrees and 60 Degrees Latitude.....	15
17 Geomagnetic Activity Variations of Density for each Model at 200 km for 0 Degrees and 60 Degrees Latitude.....	16
18 Solar Flux Variations of Density for each Model at 200 km for 0 Degrees and 60 Degrees Latitude.....	17
19 Model Density Fit Results as a Function of Altitude for Days 80 and 172.....	18
20 Density Contours as a Function of Latitude and Day for $A_p = 0$	20
21 Density Contours as a Function of Latitude and Day for $A_p = 80$	20

1. INTRODUCTION

The efforts described herein are part of a project to create, maintain and utilize an extensive neutral atmospheric density data base generated from four AFGL satellite accelerometer experiments - three on the NASA Atmosphere Explorer (AE) series, AE-C, AE-D, AE-E, and one on the Air Force S3-1 satellite. The density data were taken over a three year period from December 1973 to November 1976. The accelerometer data processing system, the analytical techniques used to extract atmospheric density from the total accelerometer output signal, and the creation of a density data base have been described previously (1,2,3).

This report describes the finalization of an extensive neutral atmospheric density data base taken from the four satellite accelerometer systems, the development of an empirical model of these data, and other aspects of data analysis support for AFGL.

Studies by AFGL scientists utilizing these results are described elsewhere (e.g., Ref. (4)).

1.1 AE/S3 Data Base

The AE/S3 density data base includes data from the elliptical orbit portions of the respective missions of the AE-C, -D, -E and S3-1 satellites. Table 1 provides orbital characteristics and dates of elliptical orbit data acquisition for each satellite. The altitudes at which data were obtained are shown in Figure 1.

Table 1. Satellite Orbital Characteristics and Data Acquisition Periods

Satellite	Launch	End Elliptical Data Acquisition	Inclination	Initial Perigee	Initial Apogee
AE-C	Dec 73	Nov 74	68°	156 km	4000 km
S3-1	Oct 74	May 75	97°	160 km	4000 km
AE-D	Oct 75	Jan 76	90°	156 km	3800 km
AE-E	Nov 75	Nov 76	20°	157 km	3000 km

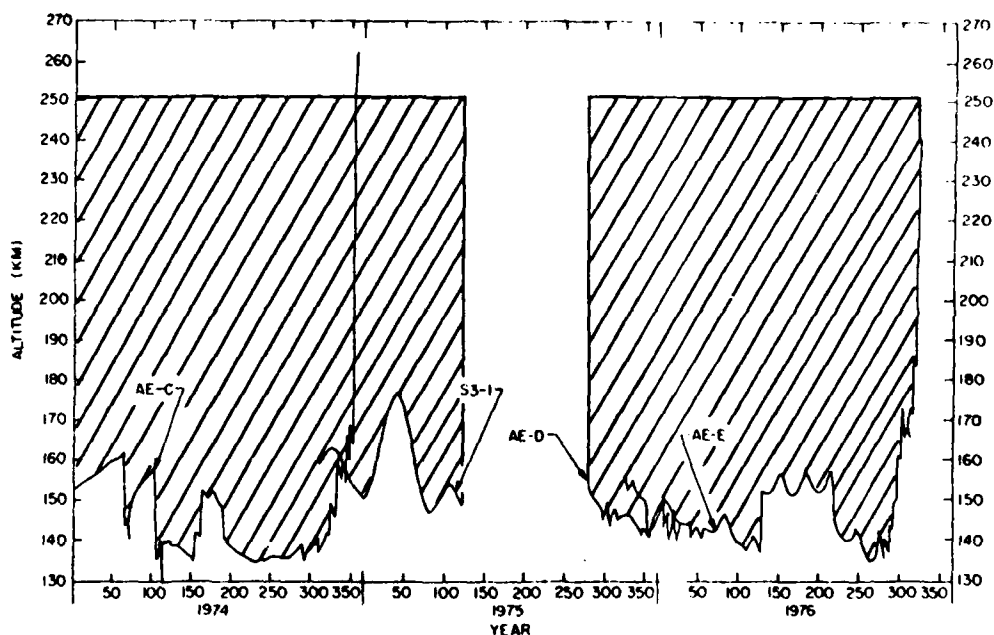


Figure 1. Distribution of Density Data

Density values were calculated at 5-km intervals and stored in the data base. Associated with each point is the corresponding satellite ephemeris data, altitude information, solar flux, Kp/Ap values, J71, J77 and MSIS atmospheric models. References (3) and (4) describe this data base in detail.

1.2 New AE-C Orbits

More than one thousand (1000) orbits of AE-C elliptical orbit data not previously processed became available and were processed under the present contract. These data were processed using the MESA data reduction system (previously described in Reference (1)), and calculated density values were stored in MESA GU and UA files.

The new AE-C density data base was then developed from the new UA density data using the techniques described in Reference (3). This data base was generated on the Sigma-9 computer and was written to magnetic tapes. These tapes were shipped to AFGL for insertion into the AE/S3 data base on the AFGL CDC 6600 computers.

To accomplish this, programs were developed to insert (i.e., merge) the new data into the existing AE-C data base for all altitudes, to quality check the resultant merged data base for duplicate data, and finally to re-merge this data base with the remainder of the AE/S3 data at all altitudes. This new composite data base makes up the present AE/S3 density data base.

1.3 Data Base Properties

Figures 2 - 6 are histograms of the data distribution as a function of geomagnetic latitude, local time, Kp index, solar flux and satellite altitude. Figure 2 shows the number of data points obtained in each 20 degree geomagnetic latitude band. Figure 3 shows the distribution of data points obtained for each hour of local time. The distribution of data with respect to geomagnetic activity is given in Figure 4. This gives the number of measurements during which the three-hourly Kp index (with 6 hr. lag) fell within a specific one unit interval. In Figure 5

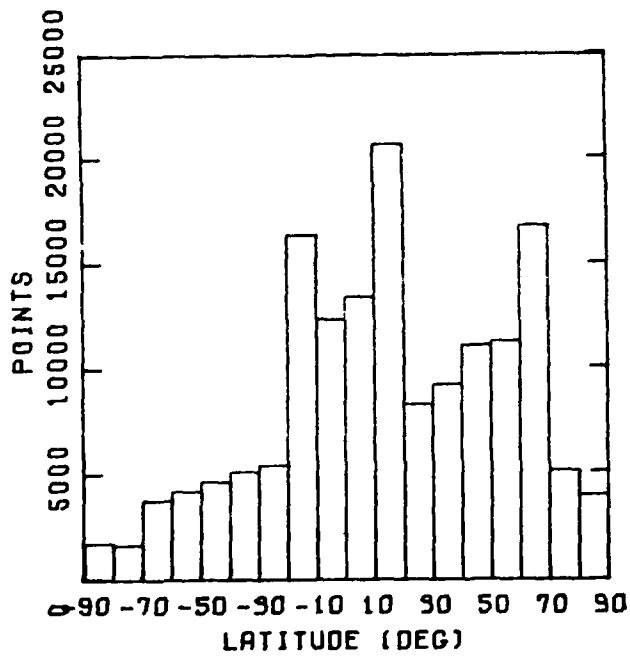


Figure 2. Data Distribution as a Function of Geomagnetic Latitude

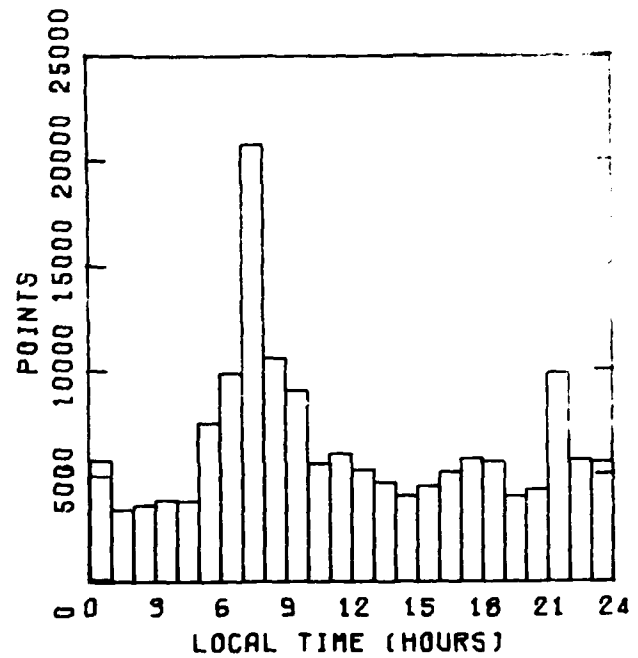


Figure 3. Data Distribution as a Function of Local Time

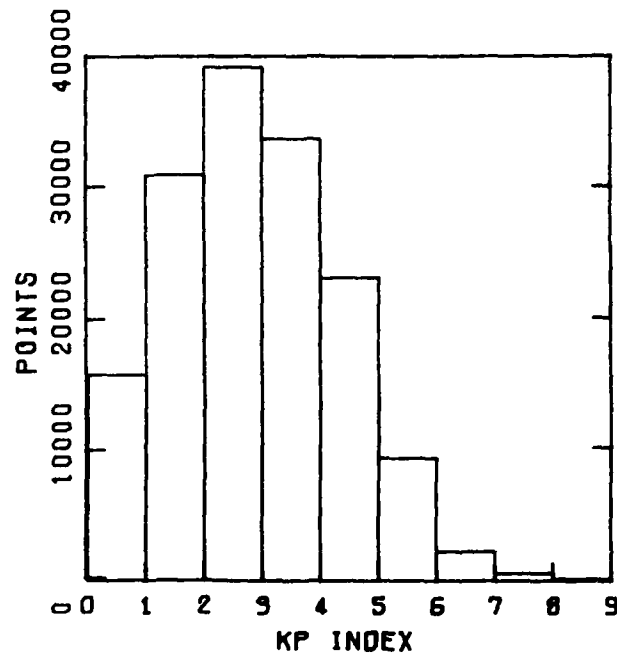


Figure 4. Data Distribution as a Function of Geomagnetic Activity

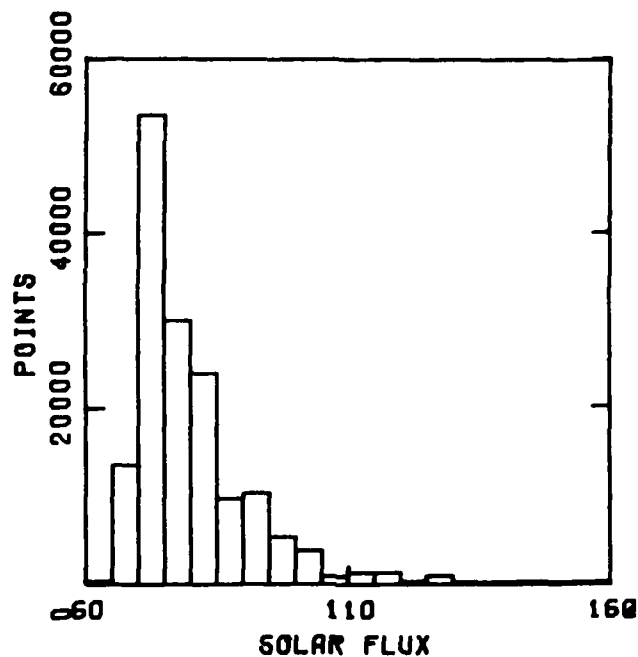


Figure 5. Data Distribution as a Function of Solar Flux

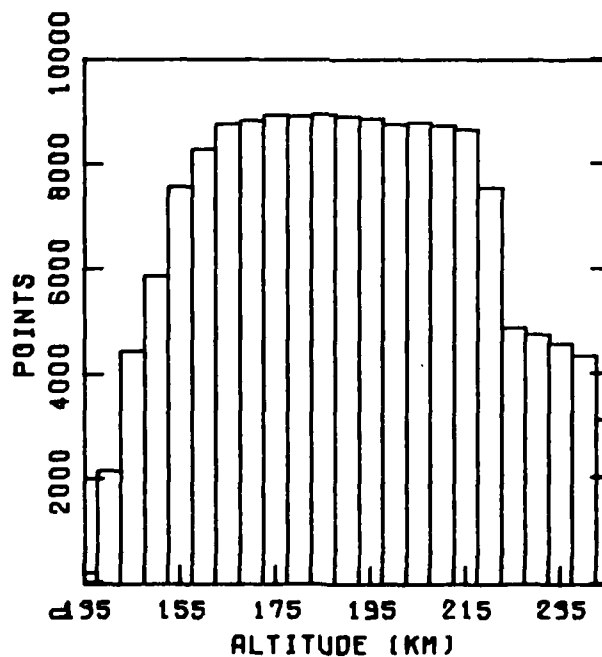


Figure 6. Data Distribution as a Function of Altitude

the number of measurements during which the daily solar flux value (with one day lag) was within specific 5 solar flux unit intervals is given. Figure 6 illustrates the number of points in each 5 km altitude file.

An example of the data base is given by showing results obtained at 180 km. Figure 7 shows the density data, corresponding solar flux values, ratio of measured density to the J71 model and the Kp index presented as a function of calendar year and GMT.

2. Model Development

2.1 J71, J77 and MSIS Comparisons

Histograms of the measured density values were provided to AFGL to permit analysis in relation to three atmospheric models - J71, J77 and MSIS. Graphical representations of frequency distributions of percent differences from the models were developed. Figures 8 - 10 display these histograms for the entire data base for each atmospheric model. Figures 11 - 13 display these histograms for 200 km data only. Frequency distributions of the data were described in terms of the mean value and the second, third and fourth moments about the mean.

2.2 Empirical Model

A multiple linear regression analysis program was utilized (3) to support the AFGL development of an empirical model of atmospheric density variations in terms of latitude, longitude, local time, geomagnetic activity, solar flux, season and semi-annual effects. This program

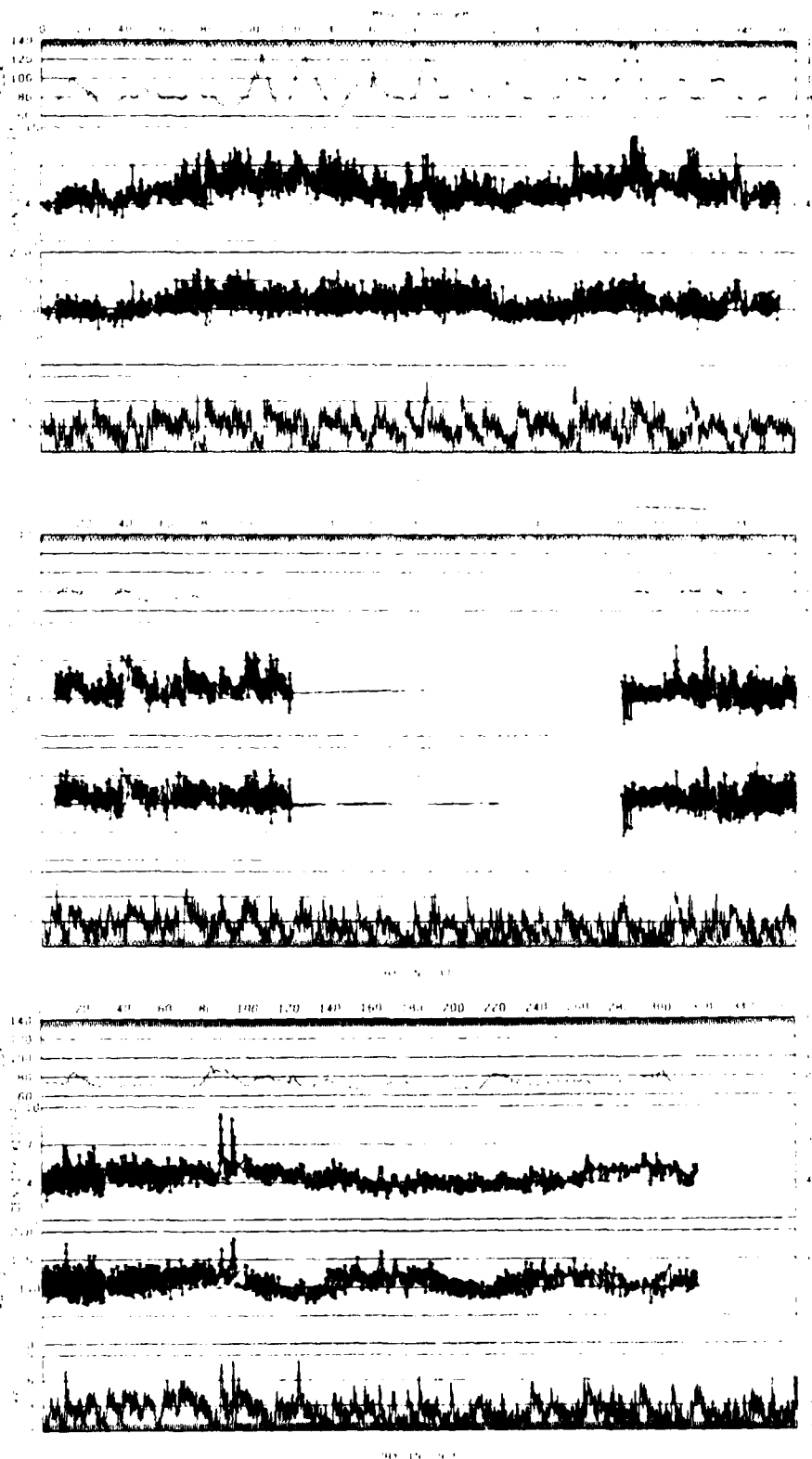


Figure 7. Data Base at 180 km: Solar Flux, Density, Ratio to J71 Model and Kp as a Function of Time

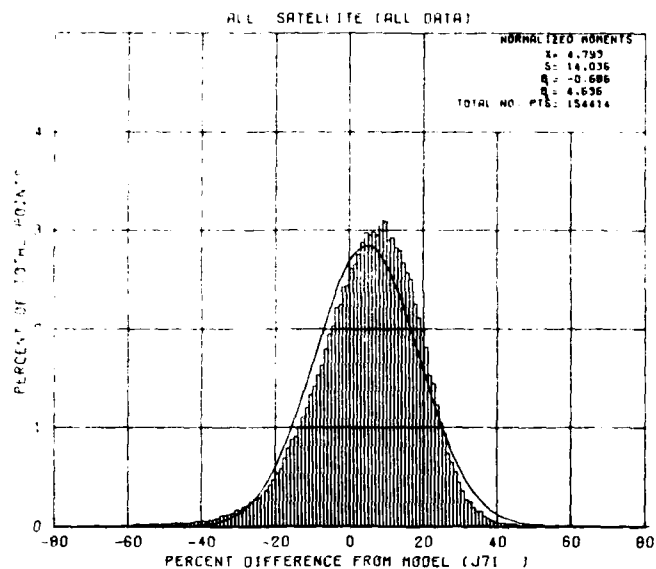


Figure 8. Frequency Distribution of Percent Differences of All Data from J71 Model

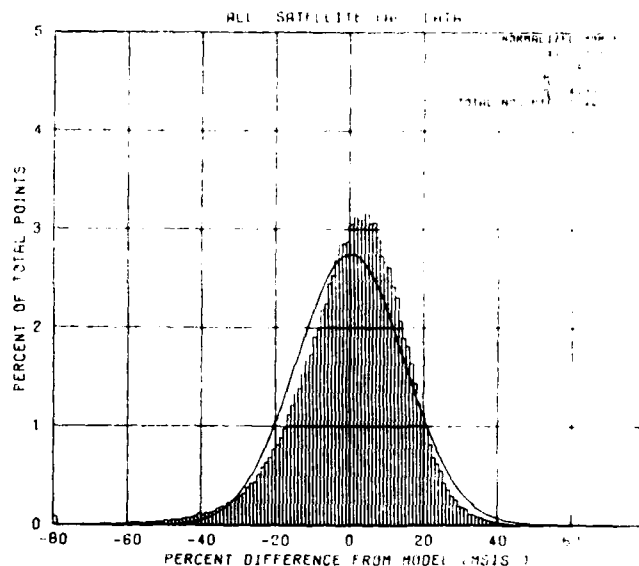


Figure 9. Frequency Distribution of Percent Differences of all Data from MSIS Model

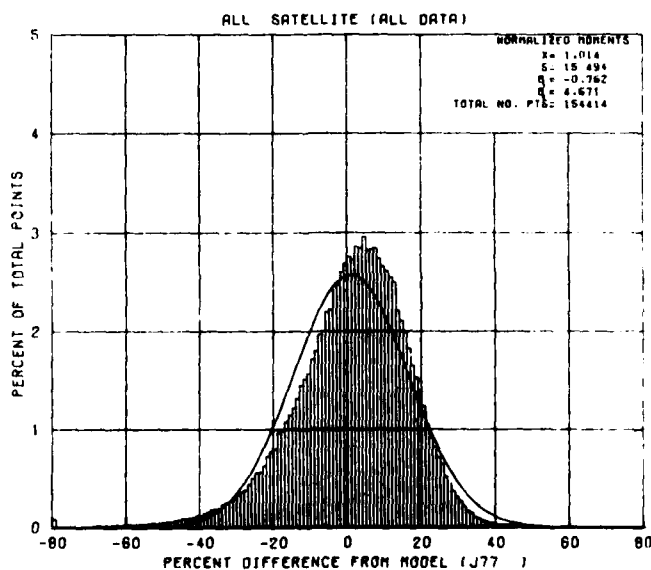


Figure 10. Frequency Distribution of Percent Differences of all Data from J77 Model

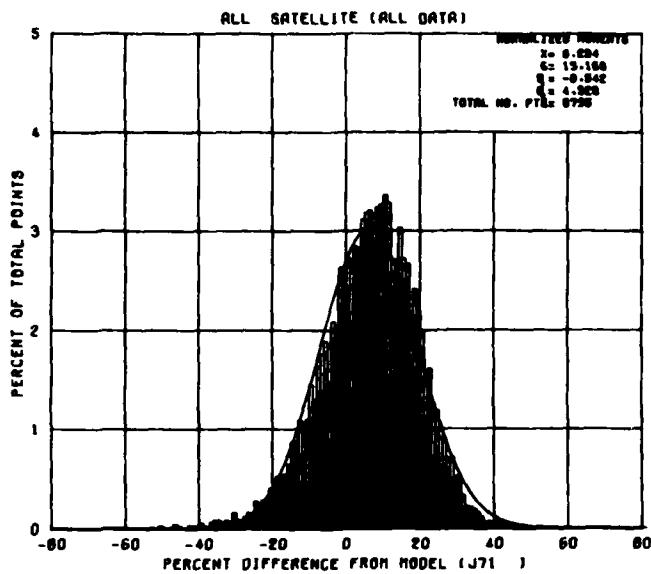


Figure 11. Frequency Distribution of Percent Differences of 200 km Data from J71 Model

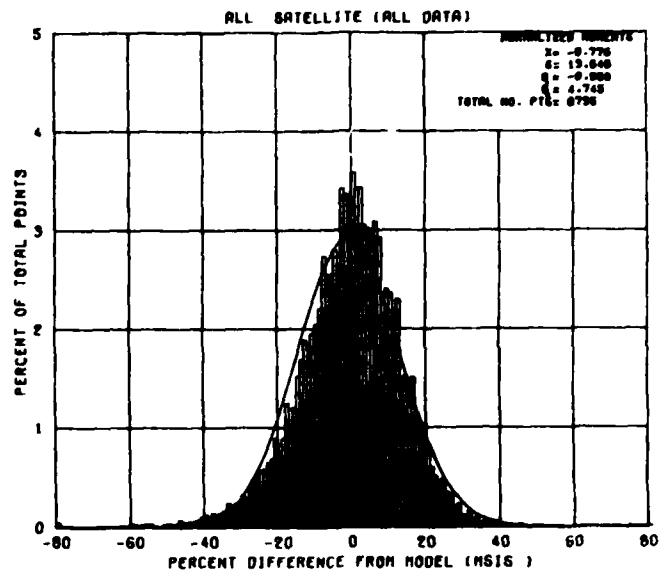


Figure 12. Frequency Distribution of Percent Differences of 200 km Data from MS16 Model

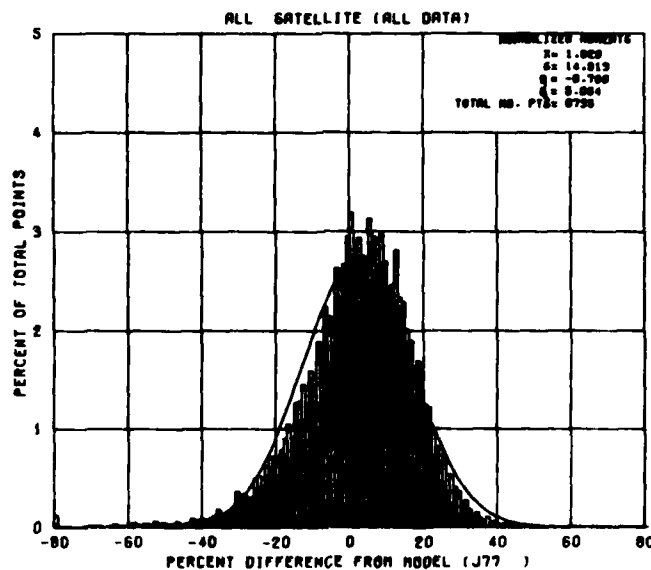


Figure 13. Frequency Distribution of Percent Differences of 200 km Data from J77 Model

was expanded to have the capability to include a much larger data base - specifically, the composite AE-C, AE-D, AE-E and S3-1 data base - and more independent variable terms. We then further expanded this program to have the capability to perform stepwise linear regression analyses on the data base to determine the amount of variation in the data which is described by each term, the significance of each term and the order which each term enters the model. Under the present configuration the multiple/stepwise regression analysis program: (a) has the capability to process a data base at least ten times larger than the original AE-C data base; (b) contains over one hundred (100) independent variables from which may be chosen the variables to be used in the particular model to be run; and (c) allows up to fifty independent variables per model.

An expanded version of the empirical model being developed in support of AFGL contains 21 independent variables and was run at each 5 km altitude from 140 to 240 km. The multiple regression program was first run to calculate the phases of the trigonometric terms, and then the stepwise regression was run to determine the order and significance of each term in the overall model. Table 2 displays statistical data related to the regression analysis including regression coefficients, stepwise correlation coefficients, and the significance and order that each term entered the analysis. Although calculated for each 5 km interval, these values are given in 20 km intervals for this report.

Table 2. Regression Analysis Results

i	F_i	a_i	a_i	a_i	a_i	a_i	a_i	ORDER ENTERED ANALYSIS					
		140km	160km	180km	200km	220km	240km	140km	160km	180km	200km	220km	240km
0	—	1.24E-12	4.48E-13	1.49E-13	3.08E-14	4.82E-15	-3.64E-15						
1	$ \theta $	0	-1.73E-15	-1.06E-15	-5.07E-16	-2.10E-16	-1.12E-16	17	10	17	18	20	
2	APLAG	0	0	0	9.18E-17	0	4.94E-17				21		16
3	$Ap_{(12)}$	5.62E-15	2.58E-15	1.41E-15	6.80E-16	4.88E-16	2.53E-16	2	6	6	1	1	1
4	$Ap_{(24)}$	3.13E-15	2.55E-15	1.12E-15	5.65E-16	3.23E-16	1.49E-16	17	1	1	9	9	13
5	F107	3.80E-15	1.20E-15	1.12E-15	7.81E-16	5.56E-16	3.12E-16	11	12	4	7	6	5
6	F107A	2.65E-14	6.83E-15	2.49E-15	1.32E-15	5.90E-16	3.75E-16	3	4	8	2	2	2
7	$\cos \omega(t_L + \phi_1)$	-1.07E-13	0	9.84E-15	1.02E-14	1.03E-14	7.55E-15	16		15	6	4	3
8	$\cos 2\omega(t_L + \phi_2)$	1.95E-13	2.22E-14	1.99E-15	4.31E-15	3.22E-15	2.65E-15	10	7	18	14	8	7
9	$\cos 3\omega(t_L + \phi_3)$	1.76E-13	1.24E-14	9.45E-15	4.34E-15	2.05E-15	1.08E-15	7	16	9	12	12	14
10	$\cos \ell(t_D + \phi_4)$	7.13E-13	1.43E-13	5.06E-14	2.15E-14	9.22E-15	6.48E-15	15	10	11	16	7	11
11	$\cos \ell(t_S + \phi_5)$	0	2.05E-14	7.37E-15	5.07E-15	2.05E-15	9.72E-16		13	16	10	11	9
12	$\sin^2 \theta$	5.73E-13	1.67E-13	1.05E-13	4.99E-14	2.23E-14	1.05E-14	14	14	5	15	15	15
13	$\cos \theta \cos \ell(t_D + \phi_6)$	0	2.11E-13	7.68E-14	3.48E-14	1.60E-14	9.57E-15		5	7	5	14	10
14	$\cos \theta \cos 2\ell(t_D + \phi_7)$	5.88E-13	9.50E-14	3.44E-14	1.78E-14	9.71E-15	6.06E-15	1	3	2	3	3	6
15	$\cos \theta \cos 3\ell(t_D + \phi_8)$	6.97E-13	3.21E-14	1.68E-14	5.21E-15	2.74E-15	1.16E-15	4	9	14	11	13	17
16	$\cos 4\omega(t_L + \phi_9)$	1.37E-13	1.42E-14	0	1.83E-15	0	4.37E-16	6	15		18		21
17	$\sin \theta \cos \ell(t_D + \phi_{10})$	8.21E-13	1.34E-13	4.22E-14	2.07E-14	1.13E-14	5.04E-15	13	2	3	4	5	8
18	$\sin \theta \cos 2\ell(t_D + \phi_{11})$	3.84E-13	6.72E-14	2.69E-14	1.27E-14	6.73E-15	3.72E-15	9	8	12	8	10	4
19	$\sin \theta \cos 3\ell(t_D + \phi_{12})$	7.44E-13	3.09E-14	1.81E-14	8.36E-15	3.45E-15	1.56E-15	8	11	13	13	16	18
20	$\sin \theta \cos 4\ell(t_D + \phi_{13})$	2.10E-13	1.30E-14	0	3.55E-15	4.03E-15	2.69E-15	5	18		19	17	12
21	$\cos \theta \cos 4\ell(t_D + \phi_{14})$	3.39E-13	0	5.53E-15	-1.87E-15	1.07E-15	-7.62E-16	12		17	20	19	19
Number of points		2145	8289	8913	8750	7553	4342						
Multiple correlation coefficient		.793	.747	.774	.796	.799	.781						

$$\text{where } \rho = a_0 + \sum_{i=1}^{21} a_i F_i$$

θ = geomagnetic latitude

APLAG = $3 + (|\theta| - 60)/12$

$Ap_{(12)}$ = 12 hr average of Ap index previous to density measurement

$Ap_{(24)}$ = 24 hr average of Ap index previous to density measurement

F107 = 10.7 cm solar flux value of previous day

F107A = 81 day centered average of F107

$\ell = 2\pi/365.2422$

t_D = day of year

$\omega = 2\pi/24$

t_L = local time in hours of day

ϕ_i = phase in
units of t

$$t_s = \begin{cases} t_D, & \theta \geq 0 \\ t_D + 182, & \theta < 0 \end{cases}$$

2.3 Results

Utilizing the regression analysis we were able to determine and display amplitude and phases of annual and diurnal variations (and their harmonics). Figures 14 - 15 display some of these results as a function of satellite altitude.

Variations due to semi-annual effects, A_p values, and solar flux information are given for 200 km data in Figures 16 - 18. Each figure displays data for latitudes of 0 and 60 degrees.

Because the empirical model is based on data at selected altitudes, it is necessary to perform some form of interpolation or fitting to obtain a continuous relation between density and altitude. We have chosen to fix (i.e., hold constant) all the parameters in the model except altitude. This generates a density value at each altitude, and then these values are fit with a function of the form:

$$d(h) = (c_0 + c_1 h + c_2 h^2 + c_3 h^3) e^{(a_0 + a_1 h)}$$

where d is the density at an altitude h .

Figure 19 displays the resultant model fit as a function of altitude for March 21 (day 80) and June 21 (day 172). The difference between the two curves is a consequence of the change in day of year. The scale height H ($\equiv -1/a_1$) changes from 25.45 km for day 80 to 24.95 km for day 172 which is consistent with the larger range of density shown. Table 3 displays the model coefficients for the curves displayed in Figure 19.

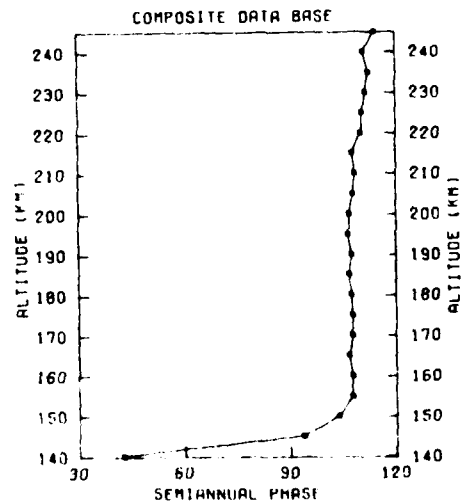
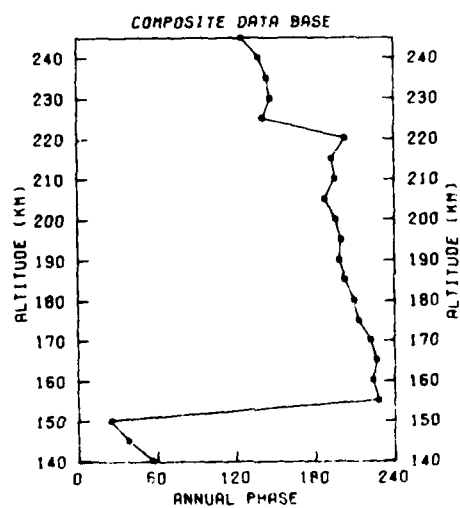
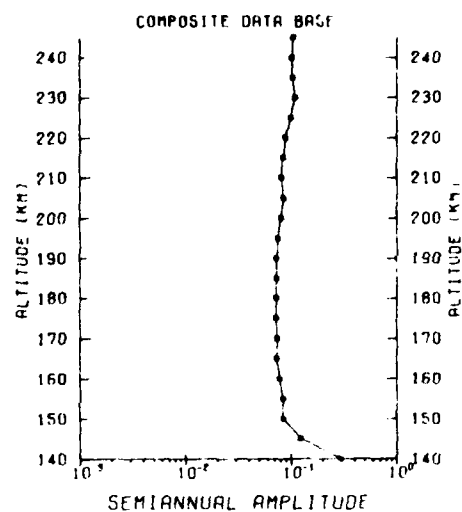
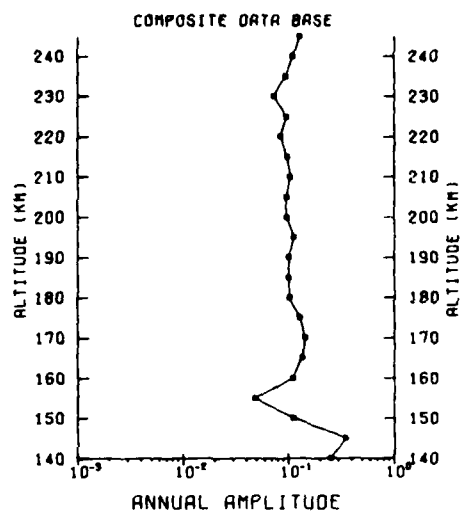


Figure 14. Amplitude and Phases of Annual and Semi-annual Variations of the Data Base

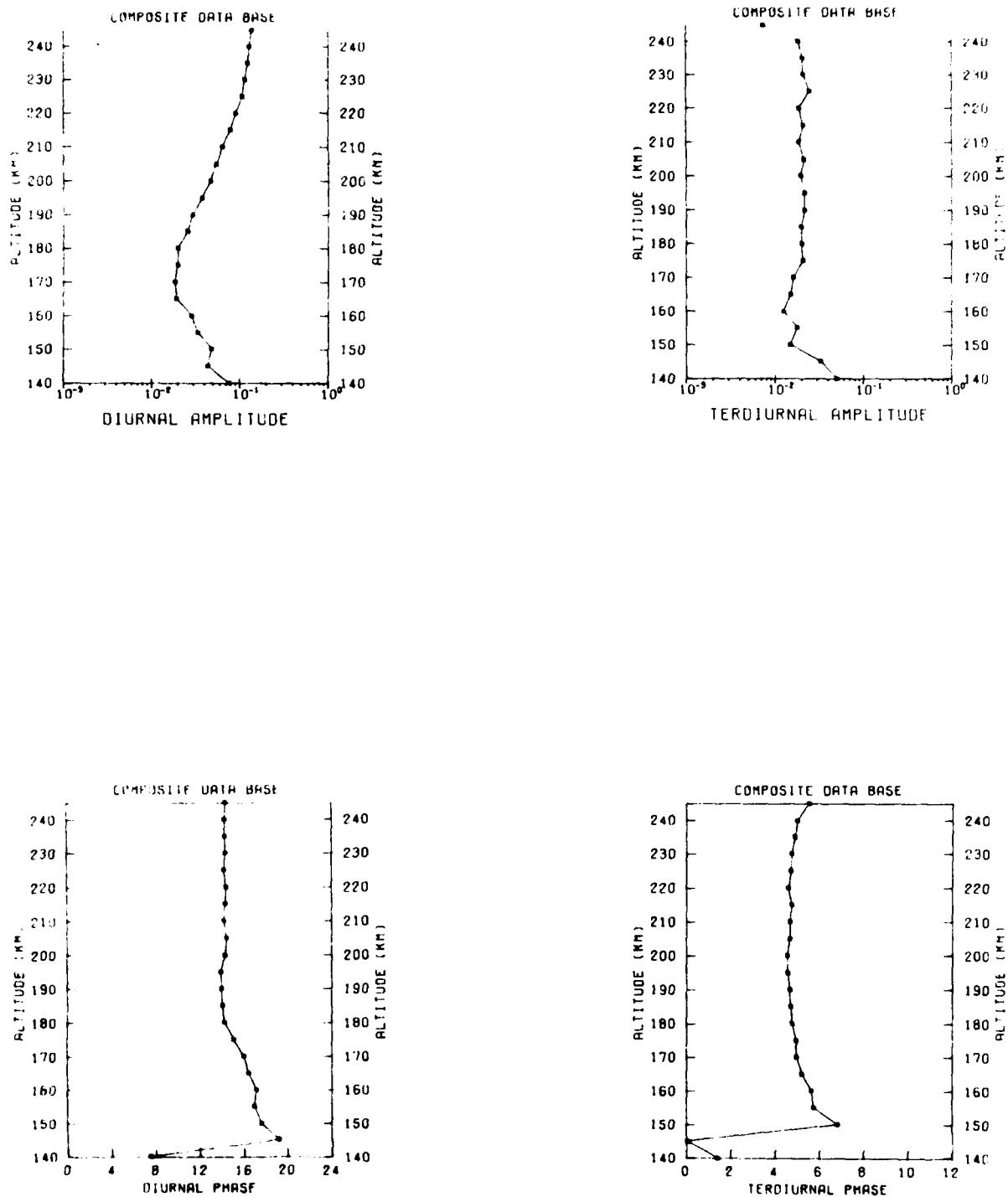


Figure 15. Amplitude and Phases of Diurnal and Terdiurnal Variations of the Data Base

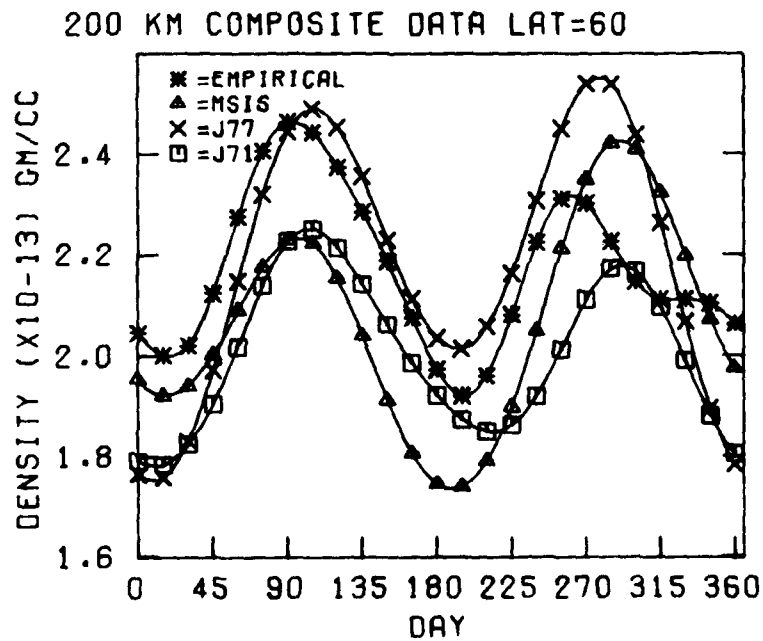
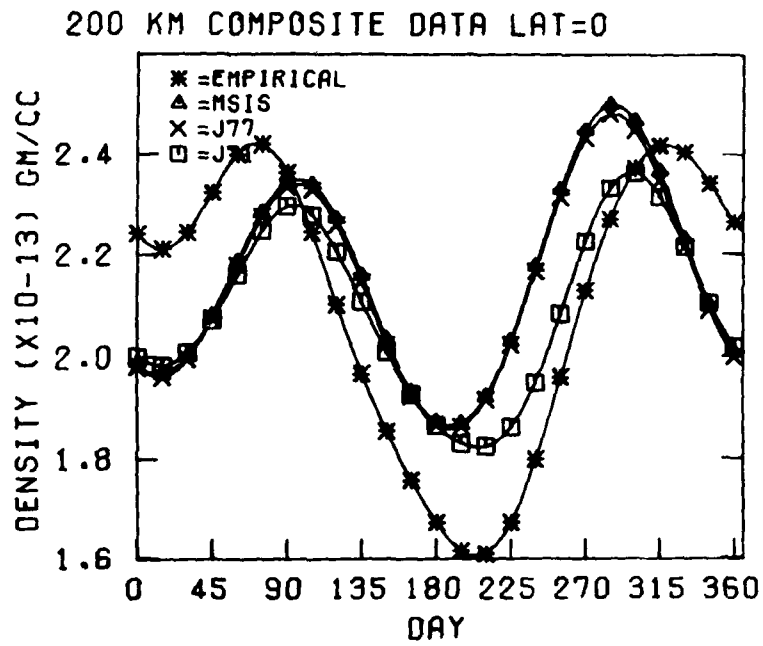


Figure 16. Semi-Annual Density Variation
for each model at 200 km for 0 degrees
and 60 degrees latitude

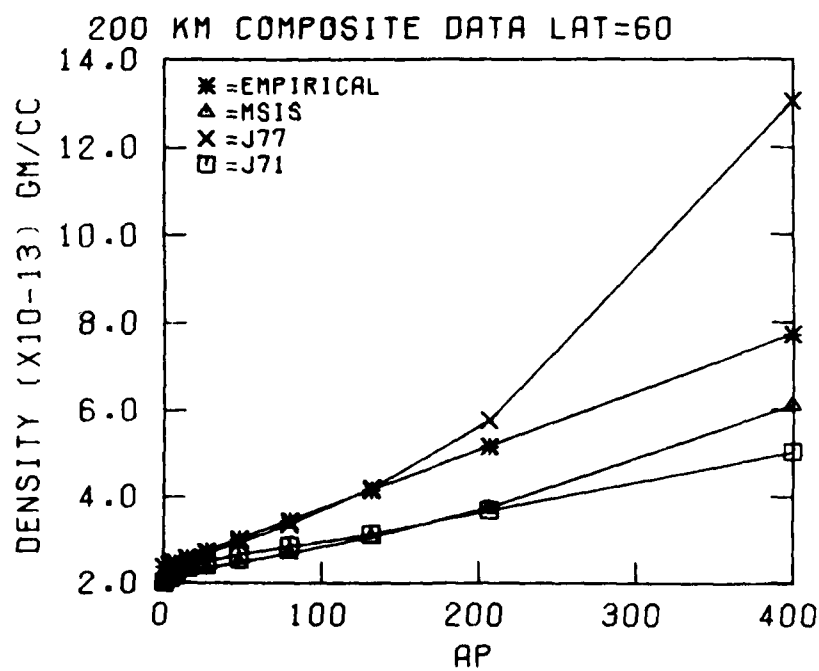
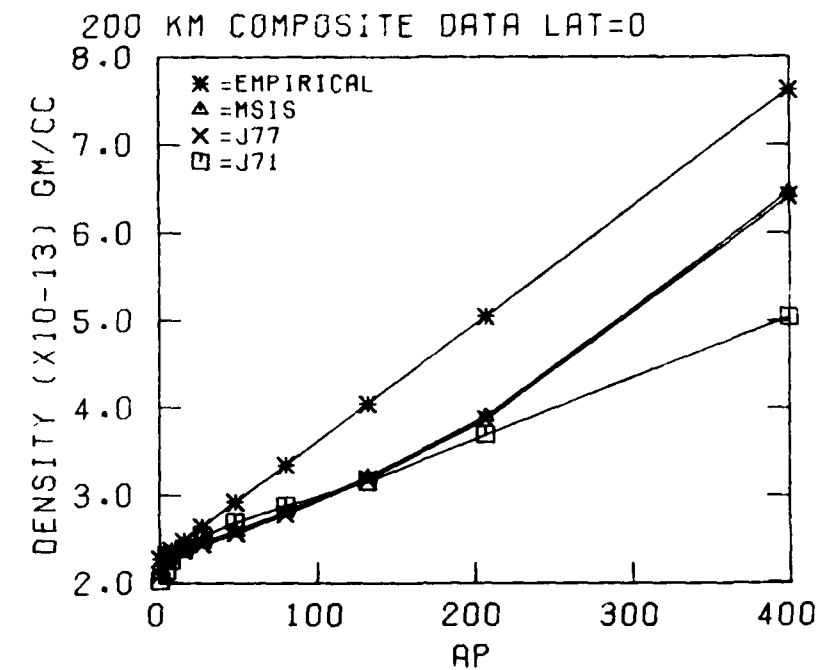


Figure 17. Geomagnetic Activity Variations of Density for each model at 200 km for 0 degrees and 60 degrees latitude

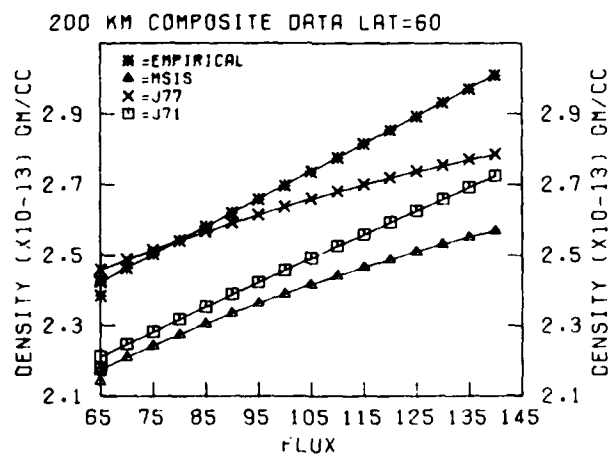
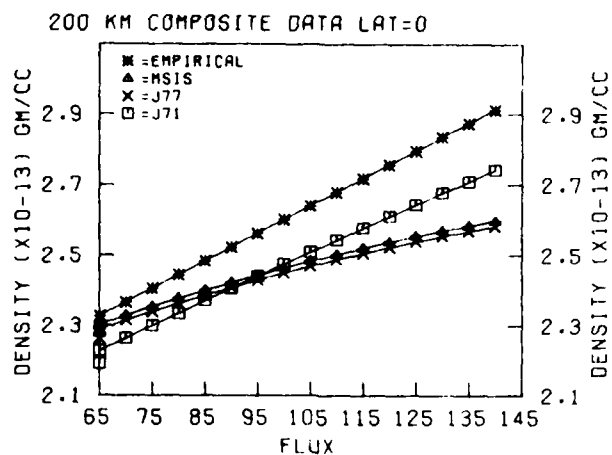


Figure 18. Solar Flux Variations of Density for each model at 200 km for 0 degrees and 60 degrees latitude

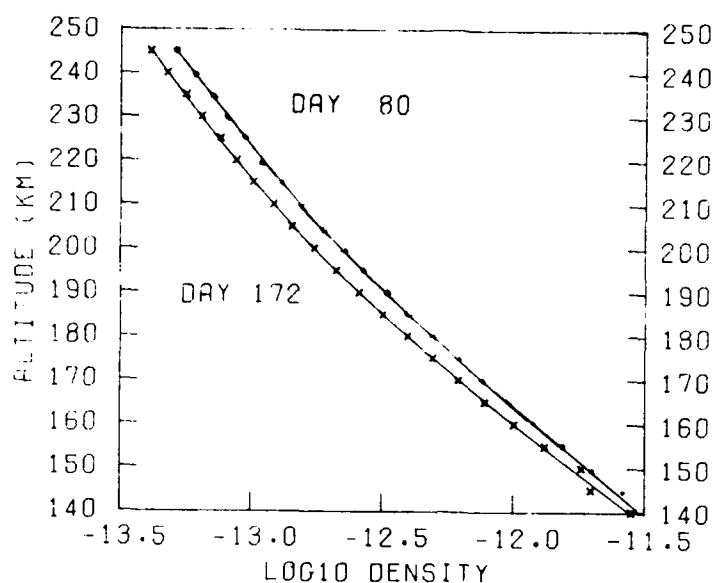


Figure 19. Model Density Fit
Results as a Function of
Altitude for Days 80 and 172.

fitting function: $d(h) = (c_0 + c_1h + c_2h^2 + c_3h^3) e^{(a_0 + a_1h)}$
 h = altitude
 d = density

calculated coefficients	day 80	day 172
C_0	3.370203E+0	5.847784E+0
C_1	-1.445794E-2	-4.957027E-2
C_2	-4.820555E-5	1.120323E-4
C_3	2.921802E-7	5.687639E-8
a_0	-2.117418E+1	-2.122403E+1
a_1	-3.929185E-2	-4.007283E-2

constant parameters

F10.7 = F10.7A = 75
 local time = 12 hrs.
 A_p = 0
 latitude = 0

Table 3. Altitude Variation of Empirical Model

In order to support studies of density variation as a function of both latitude and day of year, a set of contour plots was generated. To accomplish this all parameters except latitude and day of year were fixed. Figures 20 and 21 display density contours as a function of latitude and day of year for $A_p = 0$ and $A_p = 80$, respectively. The density values are shown in units of the ratio of the empirical model density to the actual average annual density for that altitude, with a contour interval of 0.025 in those units.

3. Other Contract Functions

3.1 EUVS Experiment Support

Utilizing our knowledge (gained in supporting the MESA accelerometer experiment) of the AE data system, the AE Sigma-9 computer system, the AE Data Management Facility (DMF) software, and the general concepts and philosophy of the AE Aeronomy Team of scientists we were required to support the efforts of the solar ultraviolet experiment (EUVS) scientists at AFGL. We utilized the remote terminal dedicated to EUVS to provide interactive on-line support. This included maintenance and execution of interactive and/or batch programs; copying various output files to the remote printers; promotion and demotion of telemetry, orbit/attitude, geophysical unit and unified abstract files; and general account and file maintenance to insure smooth execution of standard EUVS processing. In addition, manual plotting, hand calculations and file maintenance programs were written to support this requirement.

EUVS geophysical unit data were written to magnetic

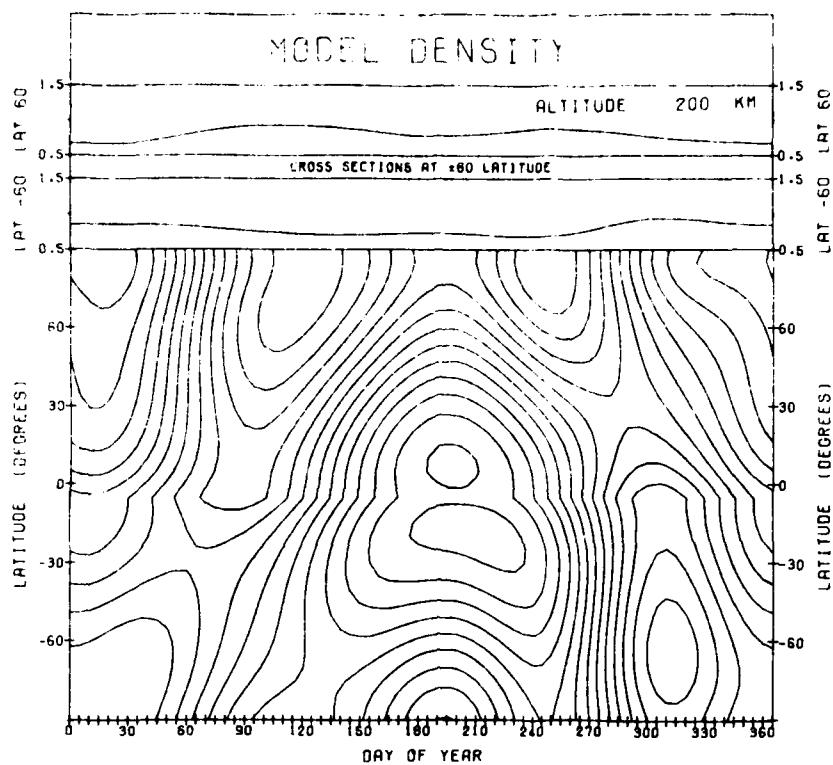


Figure 20. Density Contours as a Function of Latitude and Day for $A_p = 0$

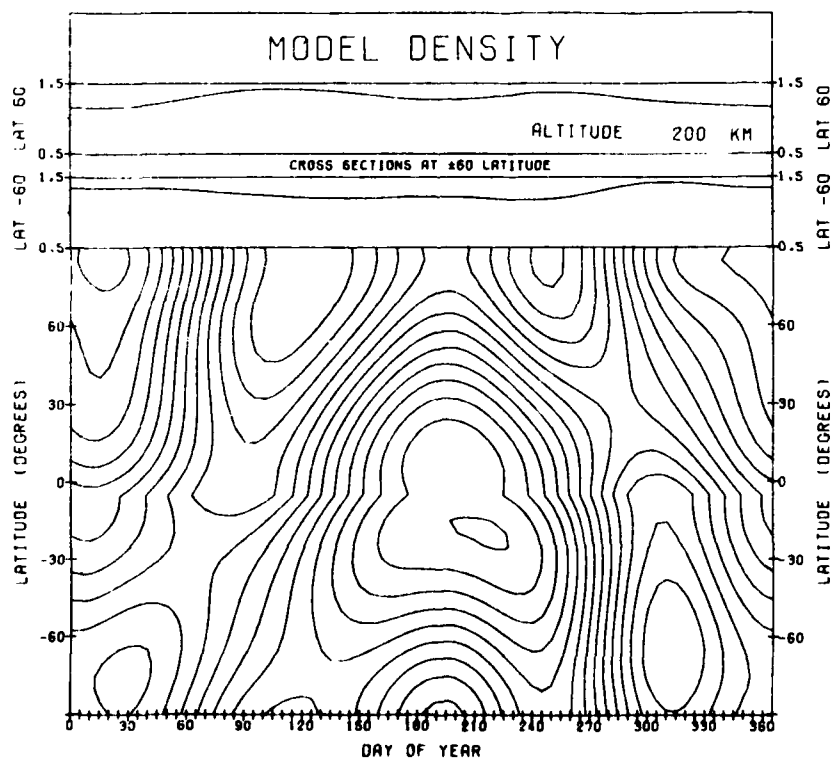


Figure 21. Density Contours as a Function of Latitude and Day for $A_p = 80$

tape on the Sigma-9 computer, and these tapes were then shipped to AFGL to be read by the CDC 6600 computer. We evaluated various tape formats and wrote programs to determine the readability of these tapes for the EUVS scientists.

3.2 AE-C Re-Entry Data

During the re-entry phase of the AE-C mission important accelerometer density data were gathered. The data were taken over the final twelve days at a rate of one orbit per day, alternating spinning and despun mode data. Seven spinning and six despun orbits were logged.

Of the seven spinning orbits two orbits contained less than three minutes of usable data; on two orbits the instrument was turned off; we were able to process data from another orbit; and two orbits were successfully processed to density values.

Of the six despun orbits one orbit contained less than three minutes of usable data, and the other five orbits were successfully processed to density values. Instrument bias values were calculated from previous high altitude circular despun data.

These re-entry data will be incorporated into the AE/S3 density data base.

3.3 Circular Orbit Processing

The objective of the AE mission was to study phenomena in the atmosphere at altitudes above 120 km. This was to be accomplished in two orbital phases: elliptic orbit and circular orbit. After the initial elliptic orbit phase was completed, AE-C and AE-E were circularized for the second phase of their mission.

For circular orbit spinning data our processing techniques to calculate density (Reference (2)) were for the

most part unchanged. For despun circular orbits, since instrument bias values are required and the satellite altitude was below the "non-drag regions" used in the elliptic orbit phase, an alternate method was required to determine bias values. We utilized the techniques described in Reference (5) to calculate bias temperature coefficients for each satellite. Circular orbit temperature data was then used to calculate instrument bias values, and filtering techniques were used to determine density values. Circular orbit density data are stored in the AE unified abstract files.

4. CONCLUSIONS

An extensive data base has been developed utilizing accelerometer measurements obtained with four low altitude satellites. Utilizing this data base an empirical model of neutral atmospheric density has been developed by multiple/stepwise linear regression techniques. It is anticipated that these techniques and results will aid in the development of improved models of the lower thermosphere.

5. ACKNOWLEDGMENT

We wish to acknowledge the support of Dr. C. John McCann for his evaluation and implementation of mathematical analyses.

6. REFERENCES

- [1] Fioretti, R.W., Ed., (1976), Atmosphere Explorer MESA Accelerometer Data Processing System, AFGL-TR-76-0137, AFGL, Massachusetts.

- [2] Noonan, J.P., Fioretti, R.W., and Hass, B., (1975), Digital Filtering Analysis Applied to the Atmosphere Explorer - C Satellite MESA Accelerometer Data, AFCRL-75-0293, AFCRL, Massachusetts.

- [3] Fioretti, R.W. and Cox, L.D., (1978), Atmosphere Explorer MESA Accelerometer Density Data Base, AFGL-TR-79-0062, AFGL, Massachusetts.

- [4] Marcos, F.A., McInerney, R.E. and Fioretti, R.W., (1978), Variability of the Lower Thermosphere Determined from Satellite Accelerometer Data, AFGL-TR-78-0134, AFGL, Massachusetts.

- [5] Marcos, F.A. and Fioretti, R.W. (1977), Orbital Bias Determination for Accelerometers on Atmosphere Explorer Satellites, AFGL-TR-77-0147, AFGL, Massachusetts.

DATE
FILMED
-8